



Preparation of microparticles through co-flowing of partially miscible liquids



Yinghe He^{a,b,*}, Sarah Battat^{b,c}, Jing Fan^{b,d}, Alireza Abbaspourrad^{b,e}, David A. Weitz^b

^a College of Science and Engineering, James Cook University, Douglas, Queensland 4811, Australia

^b School of Engineering and Applied Sciences, and Department of Physics, Harvard University, Cambridge, MA 02138, USA

^c Department of Physics, Princeton University, Jadwin Hall, Princeton, NJ 08544, USA

^d Department of Mechanical Engineering, The City College of New York, NY 10031, USA

^e Department of Food Science, Cornell University, Ithaca, NY 14853, USA

HIGHLIGHTS

- Microparticles generated by co-flowing of two partially miscible liquid phases.
- Liquid miscibility varied by changing the amount of co-solvent in inner phase.
- The miscibility influenced the flow, the particle size, distribution & morphology.
- The approach facilitated the formation of small particles with large apertures.

ARTICLE INFO

Article history:

Received 27 December 2016

Received in revised form 13 March 2017

Accepted 14 March 2017

Available online 16 March 2017

Keywords:

Microparticles
Partially miscible liquids
Controlled mixing

ABSTRACT

Monodisperse microparticles find applications in a wide range of areas. Generation of such particles of several microns in size at a large scale is a difficult task. This paper reports a proof of concept using a microfluidic device that coaxially flows partially miscible liquids for the production of microparticles. The approach makes use of both the physical forces of the process and the chemical properties of the liquid systems that allows for careful control of the mixing and droplet formation processes. Initial results show that, with this approach, particles with a reasonably narrow size distribution can be produced and liquid miscibility can be used as an additional avenue to manipulate the mean particle size and morphology.

© 2017 Elsevier B.V. All rights reserved.

1. Introduction

Monodisperse microparticles are much desired as they afford better performance control in their end use applications [1–3]. A common approach for the production of such particles is to use a monodisperse liquid-liquid dispersion as a template, which can be generated by either a chemical or a physical method, and convert the dispersed droplets into solid spheres through solvent evaporation or extraction [4,5]. Currently, chemical methods such as microemulsions make use of interfacial properties of two immiscible liquids to produce uniformly-sized particles in the nanometer range, typically less than ~800 nm, due to limitations of the chemical nature of the extremely low interfacial tension of the systems [6,7]. In contrast, physical methods such as microflu-

idic shearing [8,9] and co-flowing [10–12], as well as flow-focusing processes [13–15], manipulate physical forces of the system to produce monodisperse droplets, which are usually larger than tens of micrometers in diameter. Therefore, there exists a size gap between ~800 nm and low tens of microns in which monodisperse particles can neither be readily produced by chemical nor physical methods; however, the desired size range for some applications such as controlled drug release via intramuscular injection lies within this very gap [22,23].

By means of a physical method, droplets can be formed in two broad flow conditions or regimes termed dripping and jetting. In dripping, droplets are formed individually at the nozzle whereas in jetting they are formed at the end of a jet emitted from the nozzle as a result of Rayleigh instability [1,11,18–19]. The size of the droplets formed in the dripping regime is linearly correlated to the diameter of the injection nozzle [16,17]. The size of the droplets formed in the jetting regime, on the other hand, is determined by the diameter of the jet at the point of breakage into

* Corresponding author at: College of Science and Engineering, James Cook University, Douglas, Queensland 4811, Australia.

E-mail address: yinghe.he@jcu.edu.au (Y. He).

droplets. Two types of jets have been observed in a co-flowing arrangement. Type I jets (Jetting I) are those where the jet diameter expands, while Type II jets (Jetting II) contract, downstream. The initial diameter of the jet emitted from the nozzle is determined by the size of the injection nozzle. Making injection nozzle openings of several micrometers precisely and consistently is difficult. In addition, the use of micron-sized nozzles also causes high back pressure and blockage problems. The diameter of the jet at the point of breakage can be reduced in a co-flowing process by increasing the ratio of the outer-to-inner phase flow rates. However, there is a limit to which the jet diameter can be reduced in each flow device via this approach. When the ratio is too high, the jet flow becomes unstable and discontinuous and the droplet size becomes large again [20,21].

Largely because of its simple physical construction and well defined flow field, co-flowing microfluidics remains one of the most popular physical methods for the generation of monodisperse liquid droplets. In this arrangement, it is shown that the transition from dripping to jetting can be mapped on an inner-phase-based Webber number (We_{in}) versus an outer-phase-based Capillary number (Ca_{out}) state diagram [11]. We_{in} and Ca_{out} are defined as

$$We_{in} = \frac{\rho_{in} d_{tip} u_{in}^2}{\gamma} \quad \text{and} \quad Ca_{out} = \frac{\mu_{out} u_{out}}{\gamma} \quad (1)$$

where ρ_{in} – density of the inner phase; d_{tip} – inner diameter at the tip of the injection nozzle; u_{in} – velocity of the inner phase; γ – interfacial tension between the inner and outer phases; μ_{out} – viscosity of the outer phase; and u_{out} – velocity of the outer phase.

In theory, processes that utilize both the chemical and physical properties of the liquids should be able to produce particles of sizes in the gap region. In fact, researchers have previously attempted to utilize chemical properties of liquids in their production of particles by mixing partially miscible liquids using conventional stirring methods [24,25]. Although the approach did produce solid particles in the required size range, the size distribution was very broad. This is not unexpected considering that the flow field and hence the shear stresses and shear forces are very complex and can hardly be controlled in conventional stirring systems. The uncontrollability is further exacerbated by the diffusion of the co-solvent between the two liquid phases in the system.

This paper reports a new method for the generation of microparticles through the co-flow of partially miscible phases in a microfluidic device. This arrangement is expected to provide a more defined flow field that allows for better control of the co-solvent diffusion and droplet formation processes. The miscibility of the inner and outer phases is manipulated by altering the amount of co-solvent added to the inner phase. Initial results show that the method can yield microparticles with a much narrower size distribution than those produced by the previously reported bulk mixing approach and a mean particle diameter in the range of submicrons to hundreds of microns. More importantly, it confirms that liquid miscibility can be employed as an additional avenue to manipulate particle size and morphology.

2. Experimental

All experiments were conducted using a device made from two cylindrical glass capillary tubes (outer diameter of 1 mm) coaxially aligned in a square glass capillary (outer diameter of 1.5 mm and inner diameter of 1.05 mm). One cylindrical glass capillary was pulled using a micropipette puller (Sutter P-97 Flaming/Brown Micropipette Puller) so as to form a tapered end, from here on referred to as the injection nozzle. Two nozzle sizes were tested; their inner diameters were 20 μm and 40 μm , respectively. Fig. 1 shows the schematic of the co-flowing device.

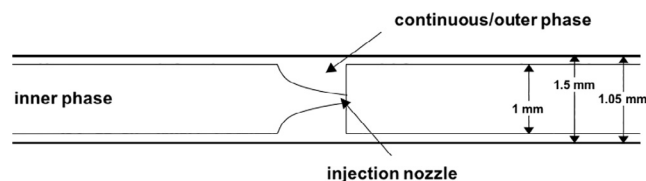


Fig. 1. Schematic of the co-flowing microfluidic device used in this investigation.

The inner phase was composed of varying amounts of polycaprolactone (PCL, average MW = 45,000) dissolved in a mixture of dichloromethane (DCM) and acetone of different proportions. The outer phase was either a 1 wt% or 5 wt% aqueous polyvinyl alcohol (PVA; MW = 13,000–23,000; degree of hydrolysis = 87%–89%) solution. In this system, DCM is immiscible with water. Acetone is completely miscible with both DCM and water and serves as the co-solvent. PCL is a solid polymer soluble only in DCM. All chemicals were Analytical Reagent grade and were purchased from Sigma-Aldrich. Milli-Q deionized water was used throughout the experiment.

Two syringe pumps (Harvard Apparatus PHD 2000) were used to pump the inner and outer phases coaxially through the capillary tubes. The inner phase was injected into the tapered capillary, while the outer phase flowed through the empty space between the injection capillary and the square glass capillary. The drop formation process under each flow condition was recorded with a high-speed camera (Phantom High-Speed Camera V7 and V9). The droplets were collected in glass vials, which were left uncovered to allow the solvent to evaporate, leading to the formation of PCL particles. The particles were washed with Milli-Q deionized water to remove PVA residue and vacuum-dried. The size and morphology of the PCL particles were determined using a scanning electron microscope (Zeiss Ultra Plus FESEM and Zeiss Supra55VP FESEM).

3. Results

3.1. State diagram

The addition of a co-solvent to the inner phase changes the physical and chemical properties of the liquid system, namely, density, viscosity, and interfacial tension. Accordingly, it is expected to alter the flow behaviour of the liquids. The instantaneous diffusion of the co-solvent (acetone) from the inner phase to the outer phase upon contact makes it impossible to measure the interfacial tension between the two phases. Nevertheless, droplet formation in this partially miscible system is observed to be similar to that in immiscible liquid systems insofar as it occurs by either dripping or jetting under all investigated flow conditions.

To compare our results with those from immiscible liquid systems, a We_{in} versus Ca_{out} state diagram was produced by assigning the same nominal value of unity (1 N/m) to the interfacial tension of all pairs of investigated liquid systems. The results are shown in Fig. 2. The outer phase of the liquid system is either a 1 wt% or a 5 wt% PVA aqueous solution and the inner phase is a DCM-acetone mixture with 0%, 40%, 60% and 90% volume fractions of acetone. Similar to the previous findings on immiscible liquid systems (Utada et al. 2007), for all pairs of the partially miscible liquids that we tested, the dripping region is always confined to the bottom-left corner of the diagram where both the viscous and inertial forces are relatively small. The significant difference (as compared to the immiscible liquid systems) is that there are multiple demarcation lines for the transition from dripping to jetting instead of a single line reported by Utada et al. (2007). As the acetone concentration in the inner phase increases, the demarcation

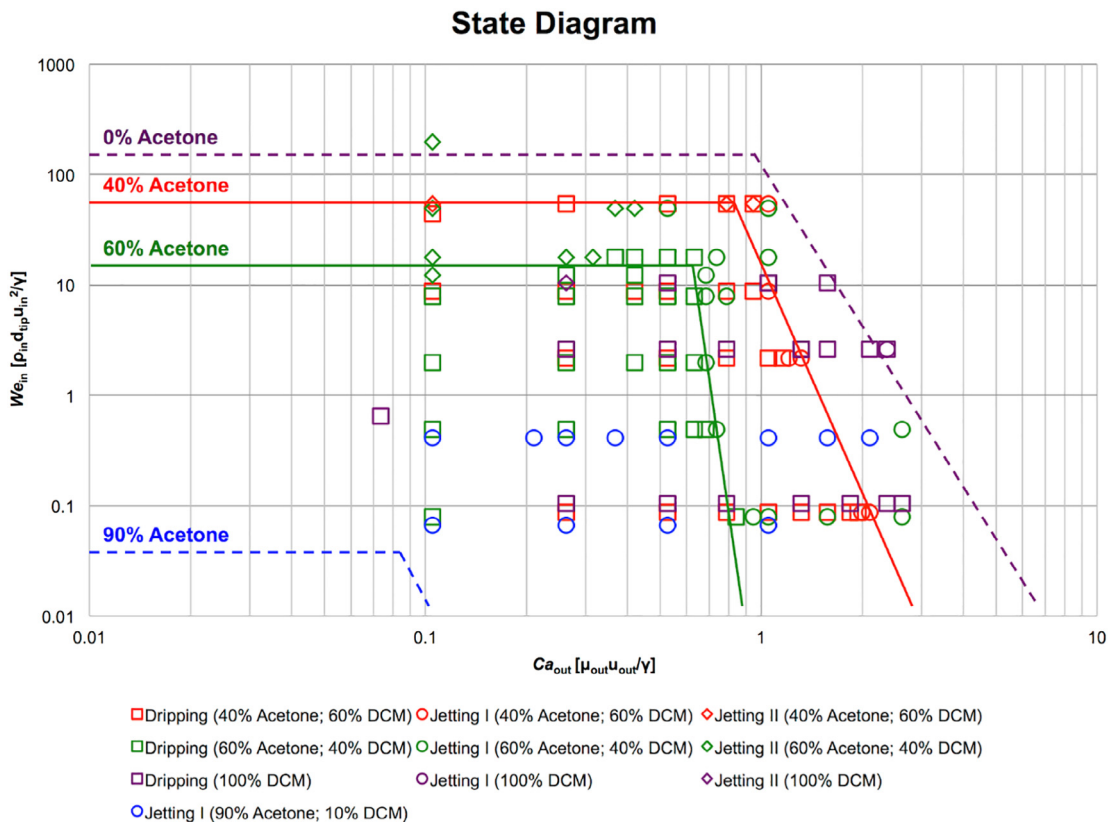


Fig. 2. We_{in} vs Ca_{out} state diagram depicting dripping, jetting I, and jetting II regimes for a co-flowing system (40 μ m injection nozzle) with a 5 wt% PVA outer phase and a 10 g/L PCL in a mixture of acetone and DCM inner phase.

lines shift towards the bottom-left corner, thereby reducing the area of the dripping region. For example, when no acetone is added to the inner phase (0%), dripping is almost always observed. In contrast, when the acetone concentration in the inner phase is 90%, only jetting is observed. This occurs because the actual interfacial tension decreases with increasing acetone concentration, making the transition from dripping to jetting possible at lower nominal We_{in} and Ca_{out} values. The transition lines for the 0% and 90% acetone cases in Fig. 2 are dashed because their positions are roughly approximated from the measured data. 0% acetone lines are drawn using the highest, and 90% acetone the lowest, We_{in} and Ca_{out} values tested in the investigation. The transition lines for the other two liquid pairs (40% and 60% acetone by volume in the inner phase) are solid because their positions are defined by the boundary at which both jetting and dripping are observed. In total, over one hundred experimental conditions were tested and the results consistently followed the trends illustrated in Fig. 2, thereby confirming the validity of this comparison.

3.2. Effect of co-solvent concentration on regime transition

The size of droplets generated in co-flowing microfluidics of immiscible liquids can be tuned by adjusting either the size of the injection nozzle or the flow conditions. With the same nozzle size, droplets formed in the jetting regime are smaller than those formed in the dripping regime. Results in Fig. 2 indicate that the presence of a co-solvent can induce a transition from dripping (in the immiscible liquid system) to jetting (in the partially miscible liquid system) under the very same flow conditions, thereby leading to a reduction in the size of the resultant droplets. Fig. 3 shows that, for two pairs of identical flow conditions, addition of

40% acetone in the inner phase indeed induces a regime change from dripping to jetting and consequently reduces the droplet size. In fact, the overall trend is that, with all other conditions remaining the same, increasing the co-solvent concentration in the inner phase decreases the mean droplet size. This finding validates the main motivation of this investigation, i.e., the viability of using a relatively large aperture (injection nozzle) to produce small particles that overcomes the blockage and high back-pressure problems associated with the use of small apertures. The smallest solid particles achieved in this investigation using a 20 μ m nozzle had a mean diameter less than 900 nm (inner phase: 90 vol% acetone, 10 g/L PCL; outer phase: 5 wt% aqueous PVA solution; flow rates: $Q_{in} = 0.2$ mL/h, $Q_{out} = 300$ mL/h).

3.3. Particle morphology and size distribution

The formation of PCL particles is a result of DCM diffusion and PCL precipitation. Due to the total miscibility of acetone with both DCM and water, the addition of acetone to the inner phase strongly influences the PCL particle formation process. Fig. 4 shows the array of PCL particles of distinct shapes and structures formed in this investigation, namely solid spheres, hollow particles and porous particles. At low acetone concentrations in the inner phase, the system behaves in a manner similar to the immiscible system thus favouring the formation of solid spheres as shown in images (A) and (B) of Fig. 4. At a high acetone concentration in the inner phase, the overall diffusion of DCM from the droplet to the outer phase is enhanced such that a DCM concentration gradient inside the droplet builds up, causing the formation of hollow spheres. Some of these hollow spheres buckle when dried in vacuum for SEM analysis, as can be seen in images (C) and (D) of Fig. 4. A high acetone

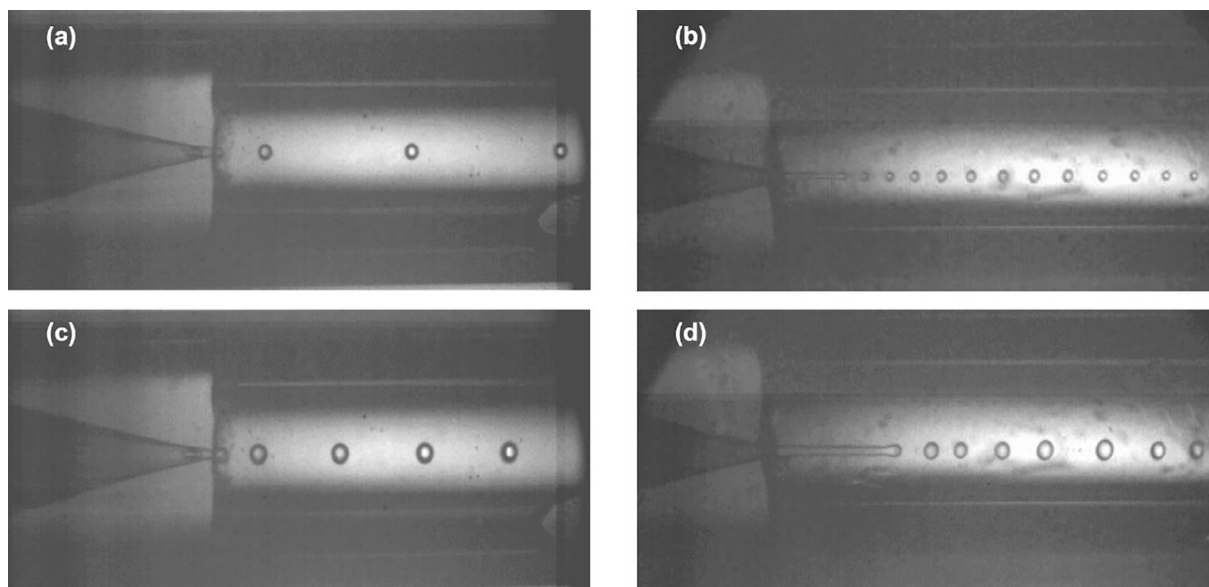


Fig. 3. High-speed video captures of co-flowing arrangements (40 μm injection nozzle) demonstrating a transition from dripping to jetting I due to the presence of acetone in the inner phase. (a, b) $Q_{\text{in}} = 1 \text{ mL/h}$, $Q_{\text{out}} = 250 \text{ mL/h}$: (a) 0%, (b) 40 vol% acetone; (c, d) $Q_{\text{in}} = 2 \text{ mL/h}$, $Q_{\text{out}} = 200 \text{ mL/h}$: (c) 0%, (d) 40 vol% acetone. The inner phase in all arrangements contains 10 g/L PCL. Outer phase is a 5 wt% aqueous PVA solution.

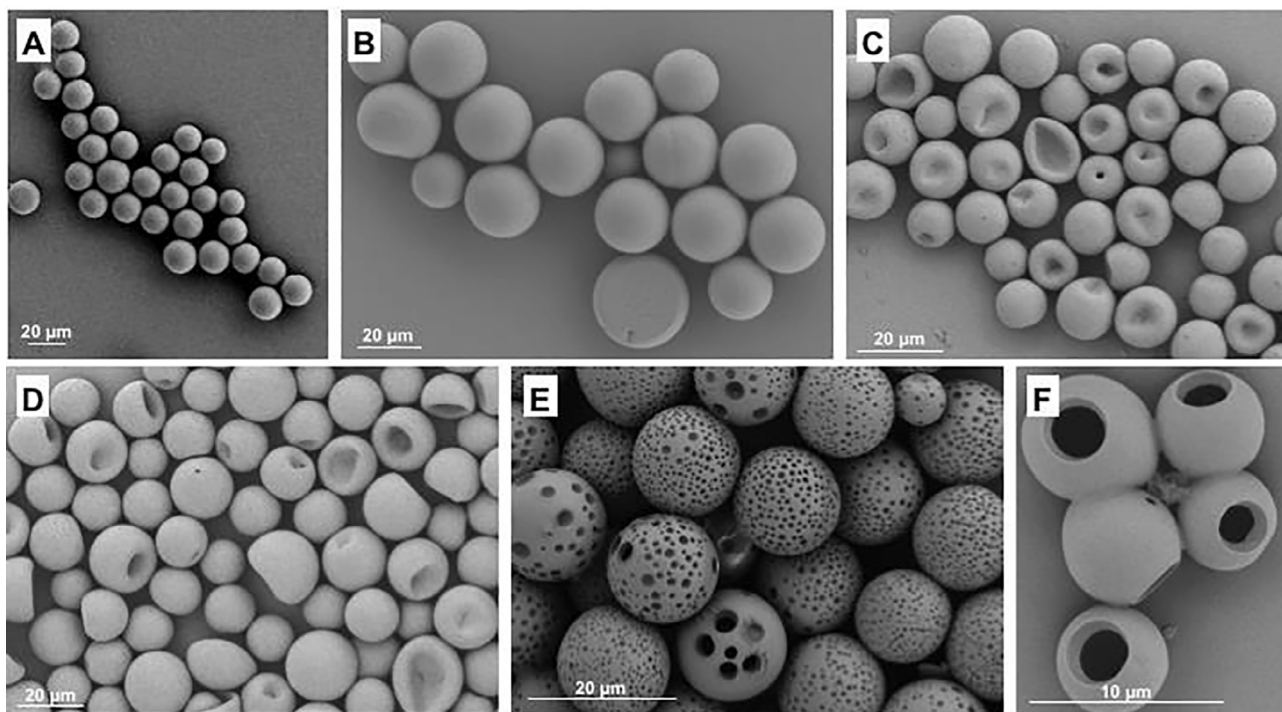


Fig. 4. SEM images of PCL particles of different morphologies. Particle generation conditions are: inner diameter of injection nozzle: (A–D) 40 μm , (D, F) 20 μm ; outer phase: (A, B) 1 wt% PVA, (C–F) 5 wt% PVA; inner phase: (A, B) 40 vol% acetone, (C–F) 90 vol% acetone; PCL concentration: (A–D) 10 g/L, (E, F) 1 g/L; flow rates: (A) $Q_{\text{in}} = 2 \text{ mL/h}$, $Q_{\text{out}} = 700 \text{ mL/h}$, (B) $Q_{\text{in}} = 2 \text{ mL/h}$, $Q_{\text{out}} = 500 \text{ mL/h}$, (C) $Q_{\text{in}} = 0.2 \text{ mL/h}$, $Q_{\text{out}} = 20 \text{ mL/h}$, (D) $Q_{\text{in}} = 0.5 \text{ mL/h}$, $Q_{\text{out}} = 70 \text{ mL/h}$, (E) $Q_{\text{in}} = 0.5 \text{ mL/h}$, $Q_{\text{out}} = 10 \text{ mL/h}$, (F) $Q_{\text{in}} = 0.5 \text{ mL/h}$, $Q_{\text{out}} = 50 \text{ mL/h}$.

concentration combined with a low PCL concentration in the inner phase results in the formation of porous PCL spheres or PCL particles riddled with very large holes as shown in images (E) and (F) of Fig. 4. A detailed mechanistic explanation on the influence of acetone in the inner phase on the particle formation is provided later in Section 4.

The addition of a co-solvent to the inner phase also influences the size uniformity of the PCL particles. Fig. 5 shows two typical

size distributions of PCL particles obtained from different acetone concentrations in the inner phase. The corresponding coefficients of variance (CVs) for these particles are 8.2% for the 40% acetone sample and 14.4% for 90% acetone sample shown in Fig. 5, respectively. Not all samples have been analysed for particle sizes in this investigation. CVs for the measured particle samples ranged from 5% to 20%, and increased with increasing acetone concentration in the inner phase.

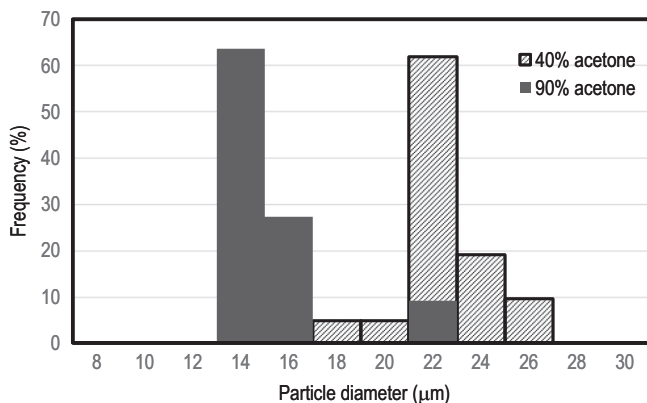


Fig. 5. Typical particle size distributions of solid PCL particles generated with 10 g/L PCL but different acetone concentrations in the inner phase using 40 μm injection nozzle. Other conditions are: 40% acetone – outer phase: 1 wt% PVA, flow rates: $Q_{\text{in}} = 2 \text{ mL/h}$, $Q_{\text{out}} = 500 \text{ mL/h}$; 90% acetone – outer phase: 5 wt% PVA, flow rates: $Q_{\text{in}} = 0.5 \text{ mL/h}$, $Q_{\text{out}} = 70 \text{ mL/h}$.

4. Discussion

In the co-flowing arrangement used in this investigation, three liquids are involved, namely DCM, acetone, and water. The solid phase (PCL) is only soluble in DCM. It precipitates when its concentration in DCM exceeds its solubility. Since each droplet results in only one particle, the mass of each PCL particle generated from this process is completely determined by the amount of PCL contained in each of the dispersed droplets. In other words, it is determined by the PCL concentration in and the size of each droplet. At each PCL concentration, PCL particle mass is linearly related to the size of the droplet. In contrast, the morphology (and the apparent particle size due to the formation of hollow and porous structures) of the PCL particles is determined by the DCM concentration profile inside the droplet at the instant of initial PCL precipitation. In turn, the DCM concentration profile is determined by the DCM diffusion from the droplet to the outer phase.

The addition of the co-solvent acetone to the inner phase has multiple effects on the PCL particle formation process in the co-flow arrangement. Firstly, it influences the droplet formation process. As seen in Section 3.1, addition of acetone in the inner phase effectively reduced the interfacial tension between the inner and outer phases. Further, it also reduced the viscosity of the inner phase as the viscosity of acetone is lower than that of DCM (0.295 mPa·s vs 0.413 mPa·s, both at 25 °C). Both factors suggest that, under the same physical and flow conditions (including the same injection nozzle), and PCL content in the inner phase, an increase in acetone content in the inner phase causes a decrease in the size of the droplets formed irrespective of whether they are formed in the dripping or jetting regime.

Secondly, the existence of acetone in the droplet after its formation changes the diffusion process of DCM from the inside of the droplet to the outer phase, thereby affecting the formation process and consequently both the apparent size and morphology of the PCL particles. The effects can be explained by the classic Whitman two-film theory [26]. In the theory, the resistance to diffusion of a species from one phase to another is assumed to occur within the film(s) where a significant concentration gradient builds up during the diffusion process. Concentrations outside the film(s) are uniform due to negligible resistance to species movement and the consequent no occurrence of net diffusion. Fig. 6 depicts a series of three schematics that qualitatively shows the time evolution of the most probable DCM and PCL concentration profiles inside the droplet, and a DCM concentration profile in the outer phase

based on the two-film theory. In each schematic, the thick black vertical line represents the interface between the droplet and the outer phase. The left side of the vertical line is the droplet while the right side is the outer aqueous phase. The shaded areas are the diffusion layers (or the films) of the droplet and the outer phase, respectively. Even though they are physically two different entities, the boundary layer of a fluid flow and the diffusion layer are related in that the thickness of the diffusion layer is strongly influenced by the hydrodynamics that each phase experiences, that is, the stronger the flow field, the thinner the diffusion layer due to the macroscopic fluid movements. Outside the diffusion layers, the DCM concentration is constant and is shown as a horizontal line in the respective phases. The solid red curves at the top of Fig. 6 represent DCM concentration profiles when no acetone is added to the inner phase while the dotted curves represent DCM concentration profiles when acetone is added. The corresponding PCL concentration profiles in each case are shown in the bottom of Fig. 6 with the same conventions. The relative vertical position of the curves represents the concentration of DCM and PCL on an arbitrary scale. The short, thin horizontal line crossing the thick vertical interface line represents the PCL saturation concentration in DCM. All conventions used in Fig. 6 are included in the bottom of Fig. 6.

Fig. 6(a) shows the concentration profiles shortly after the drop is formed and once the DCM diffusion process reaches a semi-steady state. When there is no acetone in the droplet, DCM solubility in water is low at 17.5 g/L at 25 °C and its diffusion from the droplet to the outer phase is known to be very slow due to interfacial resistance, characterised by a significant concentration decrease across the interface. The corresponding PCL concentration shows a slight increase towards the surface of the droplet. Due to the miscibility change, the addition of acetone to the inner phase is expected to increase the DCM diffusion rate from the drop to the outer phase by significantly reducing the interfacial resistance to DCM diffusion and, to a lesser extent, increasing the DCM solubility in the external phase. Consequently, a lower concentration difference across the interface and a thicker DCM diffusion layer are established inside the droplet, as shown by the lighter grey layer on the droplet side. The DCM concentration profile in the drop and outer phase in this case is shown as the dotted red curve in the top of Fig. 6(a). The corresponding PCL concentration inside the drop also shows a much more noticeable gradient over the same extended DCM diffusion layer inside the droplet, as depicted by the dotted blue curve in the bottom of Fig. 6(a).

With the continuous diffusion of acetone and DCM from the droplet to the outer phase, the bulk concentration of DCM inside the droplet decreases accompanied by a corresponding concentration profile change, as depicted in Fig. 6(b). As time proceeds, an instance will be reached where the PCL concentration at the surface of the droplet reaches saturation and starts to precipitate out while the PCL further inside the droplet remains dissolved. In other words, PCL solidification starts from the surface and moves inwards of the droplet. Depending on the extent of the concentration difference between the surface and inner part of the droplet, the resultant PCL particle can be either a solid (or filled) sphere or a hollow sphere. When the concentration difference is small, as in the case of no or a small amount of acetone added to the inner phase, the PCL inside the droplet will precipitate out soon after the surface precipitation and before the surface PCL layer becomes rigid therefore having the flexibility to change its volume and surface area until the entire sphere solidifies. In this case, the resultant PCL particles are solid spheres. Images of some typical solid/filled PCL spheres are shown in Fig. 4(A) and (B). When the concentration difference is significant, as in the case of high acetone concentrations in the inner phase, the PCL inside the droplet will precipitate out long after the surface precipitation. This will cause the formation of a hard “shell” of PCL on the surface of the original droplet

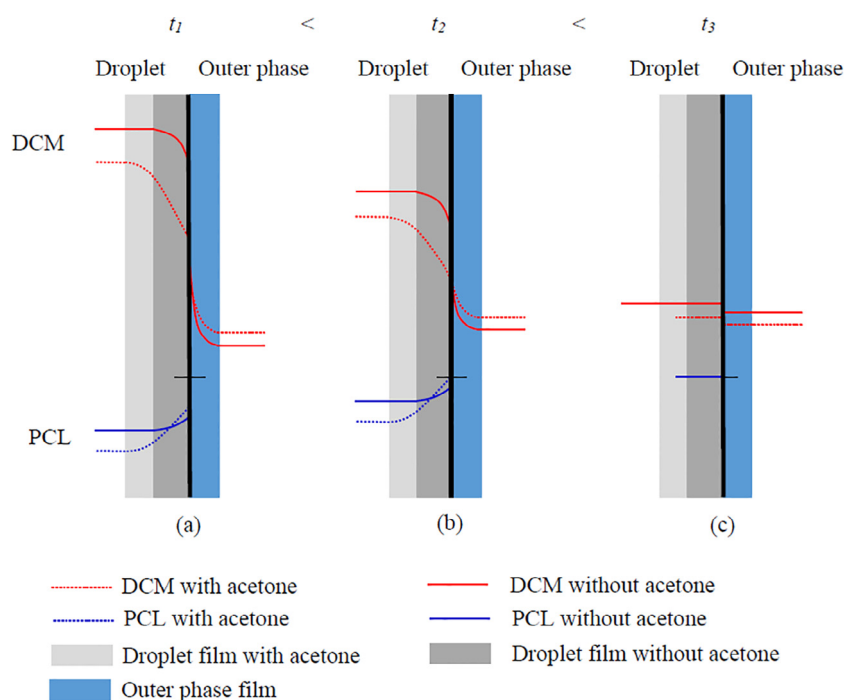


Fig. 6. Schematics showing time evolution of DCM and PCL concentrations in the droplet and outer phase with and without the co-solvent acetone in the droplet.

while a significant portion of the PCL inside the droplet still remains in the dissolved state. In this case, hollow particles will form because the diameter of the sphere is determined from the surface solidification while the droplet is still large in size from containing a high proportion of liquid DCM. Subsequent PCL precipitation occurs on the inner surface of the shell with insufficient amount of PCL available to fill the inner volume of the sphere of the rigid shell. SEM images of hollow PCL particles can be seen in Fig. 4 (C) and (D). A high DCM concentration gradient coupled with a low PCL concentration in the inner phase will result in localised PCL surface precipitation due to an insufficient amount of PCL available for the formation of a complete hard shell as well as significant DCM diffusion from the drop to the outer phase. This causes the formation of porous PCL particles and/or PCL particles with large holes, as those shown in Fig. 4(D) and (F).

In summary, the effect of acetone in the inner phase on the PCL particle morphology is qualitatively observed to be as follows: for no to low-concentrations of acetone, irrespective of PCL concentration, solid PCL particles form; for high acetone and high PCL concentrations, hollow PCL particles form; for high acetone but low PCL concentrations, porous PCL particles form.

Fig. 6(c) depicts the concentration profiles at the completion of PCL particle formation, which shows that all concentrations inside the droplet and in the outer phase have reached a constant. It should be noted that, during the PCL precipitation process, the diffusion layer thickness inside the drop changes with time. When the PCL particle solidifies completely, the diffusion layers inside the droplet and in the outer phase also disappear. They are left in Fig. 6(c) for the sole purpose of scale reference.

5. Conclusions

Results from this investigation show that the addition of a co-solvent (acetone) to the PCL-containing DCM inner phase changes the dispersion dynamics of this inner phase in the aqueous PVA outer phase in a co-flowing microfluidics arrangement. It also changes the PCL precipitation process after the dispersion. This

approach utilizes both the chemical properties of the liquids and the physical forces of the flow arrangement, resulting in the formation of PCL particles of different sizes and morphologies. An increase in the acetone concentration in the inner phase lowers the viscosity of the inner phase and the interfacial tension between the two phases, leading to a transition from dripping to jetting at lower nominal We_{in} and Ca_{out} . These changes facilitate the formation of smaller particles with the same physical device and flow conditions, validating the motivation of this investigation of using large apertures to produce monodisperse small particles. It also confirms that the amount of the co-solvent added to the inner phase can be used as an additional means for the control of PCL particle size and morphology, which is particularly useful for the production of particles in the size range from ~ 800 nm to low tens of microns. The finding has implications on all processes that produce particles of defined attributes through the liquid templating approach using immiscible liquid systems.

It must be noted that the addition of acetone to the inner phase has significant impacts on the DCM diffusion from the inner phase to the outer phase and, consequently, the droplet and PCL particle formation processes. A broader than monodisperse distribution of PCL particles generated in this investigation can be largely attributed to a lack of intentional control on the DCM diffusion during droplet formation process. Nevertheless, these particles still have much narrower size distributions than those from conventional stirring methods. Since the main objective of this investigation is a proof of concept, the conditions in this paper are by no means optimized for particle size uniformity. Optimization of flow conditions for better control over the acetone and DCM diffusion processes and hence better particle size uniformity can be the focus of future research in this area.

References

- [1] A.M. Gañán-Calvo, J.M. Montanero, L. Martín-Banderas, M. Flores-Mosquera, Building functional materials for health care and pharmacy from microfluidic principles and Flow Focusing, *Adv. Drug Deliv. Rev.* 65 (2013) 1447–1469.

- [2] T.S. Shim, S.-H. Kim, S.-M. Yang, Elaborate design strategies toward novel microcarriers for controlled encapsulation and release, *Part. Part. Syst. Charact.* 30 (2013) 9–45.
- [3] C.X. Zhao, Multiphase flow microfluidics for the production of single or multiple emulsions for drug delivery, *Adv. Drug Deliv. Rev.* 65 (2013) 1420–1446.
- [4] T. Watanabe, T. Ono, Y. Kimura, Continuous fabrication of monodisperse polylactide microspheres by droplet-to-particle technology using microfluidic emulsification and emulsion–solvent diffusion, *Soft Matter* 7 (2011) 9894–9897.
- [5] F.S. Majedi, M.M. Hasani-Sadrabadi, S.H. Emami, M.A. Shokrgozar, J.J. van Dersarl, E. Dashtimoghdam, A. Bertsch, P. Renaud, Microfluidic assisted self-assembly of chitosan based nanoparticles as drug delivery agents, *Lab Chip* 13 (2013) 204–207.
- [6] F. Ganachaud, J.L. Katz, Nanoparticles and nanocapsules created using the Ouzo effect: spontaneous emulsification as an alternative to ultrasonic and high-shear devices, *ChemPhysChem* 6 (2005) 209–216.
- [7] J.P. Rao, K.E. Geckeler, Polymer nanoparticles: preparation techniques and size-control parameters, *Prog. Polym. Sci.* 36 (2011) 887–913.
- [8] T. Nisisako, Microstructured devices for preparing controlled multiple emulsions, *Chem. Eng. Technol.* 31 (2008) 1091–1098.
- [9] C.X. Zhao, A.P.J. Middelberg, Two-phase microfluidic flows, *Chem. Eng. Sci.* 66 (2011) 1394–1411.
- [10] A.S. Utada, E. Lorenceau, D.R. Link, P.D. Kaplan, H.A. Stone, D.A. Weitz, Monodisperse double emulsions generated from a microcapillary device, *Science* 308 (2005) 537–541.
- [11] A.S. Utada, A. Fernandez-Nieves, H.A. Stone, D.A. Weitz, Dripping to jetting transitions in coflowing liquid streams, *Phys. Rev. Lett.* 99 (2007) 094502.
- [12] Z.Q. Chang, C.A. Serra, M. Bouquey, L. Prat, G. Hadziioannou, Co-axial capillaries microfluidic device for synthesizing size- and morphology-controlled polymer core-polymer shell particles, *Lab Chip* 9 (2009) 3007–3011.
- [13] A.M. Gañán-Calvo, Generation of steady liquid microthreads and micron-sized monodisperse sprays in gas streams, *Phys. Rev. Lett.* 80 (1998) 285–288.
- [14] S.L. Anna, N. Bontoux, H.A. Stone, Formation of dispersions using “flow focusing” in microchannels, *Appl. Phys. Lett.* 82 (2003) 364–366.
- [15] Y. He, Breakup of a flow-focused emulsion jet for the production of matrix-structured microcapsules, *Appl. Phys. Lett.* 91 (2007) 254112.
- [16] Q. Xu, M. Hashimoto, T.T. Dang, T. Hoare, D.S. Kohane, G.M. Whitesides, R. Langer, D.G. Anderson, Preparation of monodisperse biodegradable polymer microparticles using a microfluidic flow-focusing device for controlled drug delivery, *Small* 5 (2009) 1575–1581.
- [17] K.J. Humphry, A. Ajdari, A. Fernandez-Nieves, H.A. Stone, H.A. Stone, D.A. Weitz, Suppression of instabilities in multiphase flow by geometric confinement, *Phys. Rev. E* 79 (2009), 056310.
- [18] Z. Nie, S. Xu, M. Seo, P.C. Lewis, E. Kumacheva, Polymer particles with various shapes and morphologies produced in continuous microfluidic reactors, *J. Am. Chem. Soc.* 127 (2005) 8058–8063.
- [19] E. Castro-Hernandez, V. Gundabala, A. Fernandez-Nieves, J.M. Gordillo, Scaling the drop size in coflow experiments, *New J. Phys.* 11 (2009) 075021.
- [20] Y. He, Application of flow-focusing to the break-up of an emulsion jet for the production of matrix-structured microparticles, *Chem. Eng. Sci.* 63 (2008) 2500–2507.
- [21] J.M. Montanero, N. Rebollo-Munoz, M.A. Herrada, A.M. Gañán-Calvo, Global stability of the focusing effect of fluid jet flows, *Phys. Rev. E* 83 (2011) 036309.
- [22] X.J. Cheng, R. Liu, Y. He, A simple method for the preparation of monodisperse protein-loaded microspheres with high encapsulation efficiencies, *Eur. J. Pharm. Biopharm.* 76 (2010) 336–341.
- [23] T.X. He, Q.L. Liang, K. Zhang, V. Mu, T.T. Luo, Y.M. Wang, G.A. Luo, A modified microfluidic chip for fabrication of paclitaxel-loaded poly(L-lactic acid) microspheres, *Microfluid. Nanofluid.* 10 (2011) 1289–1298.
- [24] T. Niwa, H. Takeuchi, T. Hino, N. Kunou, Y. Kawashima, Preparations of biodegradable nanospheres of water-soluble and insoluble drugs with D,L-lactide/glycolide copolymer by a novel spontaneous emulsification solvent diffusion method, and the drug release behavior, *J. Controlled Release* 25 (1993) 89–98.
- [25] C. Wischke, S.P. Schwendeman, Principles of encapsulating hydrophobic drugs in PLA/PLGA microparticles, *Int. J. Pharm.* 364 (2008) 298–327.
- [26] W.G. Whitman, The two film theory of gas absorption, *Chem. Metall. Eng.* 29 (1923) 146–147.